Prostate Cancer Detention using Deep Learning and Traditional Techniques

Madumidha S
Assistant Professor, Information Technology, Sri Krishna College of Technology, Email: madumidha.s@skct.edu.in

Prithvi R B K
Student, Information Technology, Sri Krishna College of Technology, Email: 18tuit108@skct.edu.in

Rixon Infanton D
Student, Information Technology, Sri Krishna College of Technology, Email: 18tuit116@skct.edu.in

Abstract

Prostate disease (PCa) is a serious sort of malignant growth and makes significant passing among men due its poor demonstrative framework. The pictures got from patients with carcinoma comprise of intricate and fundamental highlights that can't be extricated promptly by customary symptomatic procedures. There have been only very few assessments that have portrayed the periods of partition of prostate CT pictures. As needs be, in this article, we propose an Ensembled Transfer Learning (ETL) design to arrange well, moderate and deficient isolated prostate CT pictures.

Keywords: *prostate cancer, image processing, k-means clustering, cell division, segmentation.*

1. Introduction

The prostate is an organ which is only located in men, below the gall bladder. It is a vital organ in the male anatomy as it is used mainly for reproduction. The prostate cancer is one of the deadliest cancers in the world, which constitutes for fourth largest number of deaths among men by cancer. It grows slowly and it is very difficult to identify it through symptoms. It is often deadly in the final stages. The technique used in this project is called the picture handling. What this technique does is it uses machine learning to separate the important information from the pictures of the prostate and the cells around it.

2. Types of image processing

The strategy that is implemented in this project is advanced image processing. Simple image processing can be used only for physical entities like documents or paper. Image processing methods are really of great help when it comes to segmenting the image and acquiring the necessary details in the image so that the problems can be easily identified by the computer without the help of humans, by the means of machine learning and deep learning. Usually when it comes to image processing, the data goes through three stages that are typical in almost every image processing projects. The three stages are pre-handling, improvement and data extraction.

3. Application

Safeguard reconnaissance - Aerial observation techniques are used proficiently to watch out for safety of the land and seas. This application has become very popular and is used to find the sorts the position and arrangement of maritime vessels that are in the sea. Biomedical Imaging procedures - For clinical determination, various kinds of imaging apparatuses, for example, X-beam, Ultrasound, PC supported tomography (CT) and so forth are utilized. The outlines of X-beam, MRI, and PC helped tomography (CT) are given beneath. There are many other applications involved with this image processing.

4. Biomedical image processing

Biomedical image processing mainly focuses on the minute details of the photos that are used as input for helpful purposes. Biomedical image processing machinery often use x-rays, ultrasound, MRI or endoscopy to visualize the current status of an organ or a tissue which is used to analyze a patient after some kind of therapy and symptomatic assessment. The technology behind the medical instruments and the programming behind it are being developed and improved drastically since the invention of x-rays in 1895. For example, the present day x-rays are so efficient that within milliseconds you could get the perfect picture of the body and organs. The picture quality is also vastly improved compared to the first x-ray.

5. Cell segmentation

Cell segmentation is the process of splitting an image which is microscopic in size, into a number of segments to identify cells. It is a basic process and a fundamental step in many types of biomedical studies and it is considered to be a highlight in cellular based research. Cell segmentation is used to find border of each and every cell and map the number of cells present in the particular image. With the help of new technological advances in the field of light microscopy, cell segmentation process is becoming simpler day by day. The images provided below denote the difficulty in cell segmentation.

Figure1.Easy Image Figure2.Difficult Image

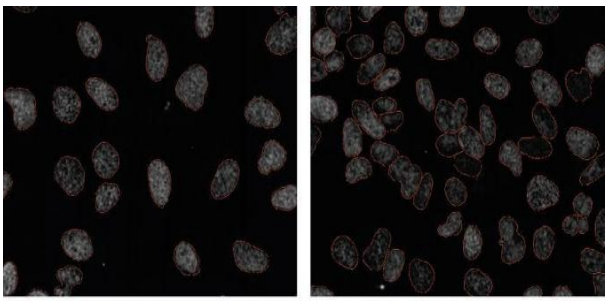

6. Cell counting

Cell counting is any of different techniques for the counting or comparative measurement of cells in the existence sciences, including clinical determination and treatment. It is a significant subset of cytometry, with applications in research and clinical practice. For instance, the total blood count can assist a doctor with deciding why a patient feels unwell and how to help. Cell counts inside fluid media are typically communicated as various cells per unit of volume, hence communicating a fixation (for instance, 5,000 cells for each milliliter). For microbial science, cell culture and a considerable lot of the applications that require utilization of cell suspensions, deciding the convergence of cells is essential. The gadget utilized for deciding the quantity of cells per unit volume of a suspension is known as an including chamber.

7. Related work

The primary objective is to identify the cells which are cancerous in the prostate with the help of trained artificial intelligence calculators like K-Means with Expectation Maximization (EM), Naive Bayes and the boundaries like F-Score, Recall and Precision. As microscopic pictures can have different staining designs, pre-processing of pictures might be crucial to identify the number of cells and count them. The grouping of cells is made by partitioning

the full microscopic image into a number of patches. These patches are then distributed to the foundation for a closer view.

Rashidul Alam Mahumudet.al., has proposed that cancer is a significant general well being worry as far as grimness and mortality around the world. A few sorts of malignant growth patients experience the ill effects of persistent co-morbid conditions that are quite difficult for therapy and disease the executives. An enormous number of disease patients experience an outrageous weight of constant co-morbid conditions and the various components of these in malignant growth survivors can possibly influence the direction of their malignant growth trouble. It is additionally critical for medical care suppliers, including actual specialists and oncologists, who should deal with the extraordinary issues that challenge this populace and who ought to advocate for counteraction and proof based medications. This study will analyze the longitudinal idea of ongoing co-morbid states of disease patients. All the more explicitly, the review proposes to foster a superior comprehension of the longitudinal dispersion of persistent comorbidity status among malignant growth patients as well as its effect over the long haul. This study supplements and adds to this strand of progressing malignant growth examination to increment mindfulness and further develop general well being practice among victims and survivors, and to gauge sway.

8. Proposed system

We use K-Means Clustering to segment the picture and find the edges of the cells. This method is done using the histograms which are the result of picture force. The picture force usually makes a vector space and tries to find if there is any grouping of cells in the picture. Even though, fluorescence magnifying instruments display multi-layered datasets, handling them is really a very difficult task and sometimes if the mistakes are committed, it might be expensive to recover the original process. Therefore, a planned execution is really necessary if you are about to use fluorescent magnifying instruments. The main downside of this is they are really expensive.

Explicit recognition of neurotic changes in cells requires the exact estimation of mathematical boundaries. Past exploration has shown that mathematical elements, like shape and region, demonstrate changes in the cell during apoptosis. As a forerunner to mathematical examination, division is regularly expected in the primary handling step. Cell picture division is trying because of the complexly structured cells, enlighten reflection, and innate microscopy commotions. The trademark issues incorporate unfortunate differentiation between cell dark levels and foundation, countless cells viewed in solitude, and overabundance of similarity in cell pictures because of instantaneous staining among cells and tissues. Ordinarily, picture division calculations depend on neighborhood picture data, including edge or slope, level set histogram groups and earlier information.

The division strategies have always been very essential in clinical imaging applications. The calculations done by these division strategies are being used in pictures of cells which assimilate machine learning and groupings based on histograms. Unaided machine learning can be trained very efficiently to follow these division strategies accurately and precisely to identify those cancerous cells by drawing boundaries.

Once in a while, strategies are chosen in view of instinct; e.g., Otsu's edge is utilized comprehensively in cores picture division. Additionally, no extensively satisfactory technique can address the cores and cell picture division issues in a different scope of uses precisely and heartily. As of late, a few engineered and benchmark cell picture information have been made freely accessible.

In this work, we present and assess the presentation of a few solo information mining strategies in cell picture division. It ought to be noticed that the division calculations are commonplace agents of strategies in view of histogram, model, limit, and dynamic shape. We just spotlight on division strategies utilizing low-level picture data, like pixel force and picture angle. GMAC addresses the level set innovations and the snake. The outcomes introduced in this paper can direct area clients to choose appropriate division strategies in clinical imaging applications.

9. K-means clustering

As mentioned in the heading "Proposed system", we utilize K-means clustering to find the groups in a labeled set of data which are not conclusively labeled or not labeled properly. This method is done utilizing the histogram of power of picture. "ci" define the centroids,

$$ci: = \arg\min (dis (x_i - \mu_i)$$

The centroids for every cluster can be calculated with the below equation:

$$\mu_i: = \frac{\sum_{i=1}^{r}\{ci=j\}x_i}{\sum_{i=1}^{r}\{ci=j\}}$$

In the above equation, r is the size of the picture, I denotes all the forces, μi are the centroids powers and j repeats over all centroids. What is proposed is that a change of work in the Tr (I) = Ir for the above calculation to carry out k-means division in cell picture I, where γ is positive steadiness.

10. EM method

What Expectation Maximization (EM) algorithm does is that it almost concludes that most images have different grey-levels at different places of the images. They can be verified using the data from cancer institutes. The purpose of EM algorithm is to find the parameters of maximum approximates in a particular situation. The two steps that are involved in using the EM algorithm are maximization and expectation. The different mixture of probability density functions is given down below,

$$P(x_i)=\sum_{j=1}^{k} \alpha_j \, p_j(x_j:\theta_j)$$

In the equation mentioned above, $\sum_{j=1}^{k} \alpha_j \, p_j(x_j:\theta_j)$ is the density function with parameter set θ_j. In practicality, GMM is used by many people and it has a total of two parameters of, which are μ_j and $\sum j$.

If we assume that θ_j is estimated value of parameters $\theta_j = (\mu_j, \sum j)$, obtained at the step that is at the top, then again it is obtained at the above step, then θ_j can be received continuously. Framework of this algorithm is given below:

$$\alpha_j^{t+1}=\frac{1}{r} \sum_{i=1}^{r} \alpha_{ij}^{t}$$

$$\mu_j^{t+1}=\frac{\sum_{i=1}^{r} \alpha_{ijx_i}^{t}}{\sum_{i=1}^{r} \alpha_{ij}^{t}}$$

$$\sum_{j}^{t+1} = \frac{\sum_{i=1}^{r} \alpha_{ij}^{t} \left[\left(x_{i-}\mu_j^{t+1}\right)\left(x_{i-}\mu_j^{t}\right)\right]}{\sum_{i=1}^{r} \alpha_{ij}^{t}}$$

$$\alpha_{ij}^{t}=\frac{\alpha_j^t p(x_i;\mu_j^t,\sum_j t)}{\sum_{j=1}^{k} \alpha_j^t p(x_i;\mu_j^t,\sum_j p)}$$

These above equations denote that the parameters that are already estimated, of the density function, are updated based on the average of the different pixel values. The total expectation maximization cycle starts from $\theta_j^o = (\mu_j^0, \sum_j 0)$ and updates the parameters. Then, the final parameters $\theta_j^o = (\mu_j^{EM}, \sum_j EM)$ are applied in the splitting process of the images, by tagging the pixels. The pixel *xi* is tagged using the equation down below,

$$areg\ max_{j\frac{\exp(-0.5}{\sum_j EM}}\left(x_{i-}\mu_j^{EM}\right)\sum_j EM\left(x_{i-}\mu_j^{EM}\right)$$

11. Threshold-based segmentation

This method splits a particular photo into different understandable regions, which are done with the existing threshold values. Threshold values are in the form of integers in the range from 0 to L-1, where L-1 is defined as the maximum intensity value. It is usually used to make a photo split into two important parts: the object and background. The threshold segmentation equation is given below:

$$I_B\ (x, y) = \begin{cases} if I(x,y) > T \\ 0, if I(x,y) < T \end{cases}$$

In the above equation, the segmentation resultant is I_B. Otsu proposed the most popular threshold method. It finds the correct threshold value T (optimal threshold) among from the values of 0 to L-1, then a value is chosen that produces the least variance σ^2within as the best threshold value. In the equation down below, we can find the optimal threshold value:

$$\sigma^2\text{Within}\ (T_{opt}) = min_{0<T<l-1}[\ \sigma^2\text{Within (T)}]$$

Variances σ^2 is given below:

$$\sigma^2 = \ \sigma^2\text{within(T)} + \ \sigma^2\ \text{between(T)}$$

Otsu shows that $max\ _{0<T<l-1}[\ \sigma^2$between (T)] therefore, T is obtained by the following alternative process down below:

$$\sigma^2\text{Between}\ (T_{opt}) = max\ _{0<T<l-1}[\ \sigma^2\text{between (T)}]$$

Theoretically, σ^2Between(T) is expressed in the following

$$\sigma^2\text{Between(T)} = \omega_1(\text{T})\ \omega_2(\text{T})\ (\mu_1(\text{T}) - \mu_2(\text{T}))^2$$

where ω_i (T)=$\sum_{i=1}^{T} h(i)$ are the probabilities of the clusters, and $\mu_i(T)_{i=1,2}$ are the cluster means $\omega_i(T)_{i=1,2}$ and $\mu_i(T)_{i=1,2}$ can be approximated using the histogram h(x) as follows:

$$\omega_1(T)_{i=1,2}=\sum_{i=1}^{T} h(i)$$

$$\omega_2(T)_{i=1,2}=\sum_{i=T+1}^{L-1} h(i)$$

$$\mu_1(\text{T})=\frac{\sum_{i=0}^{T} i.h(i)}{\omega_1}$$

$$\mu_2(\text{T})=\frac{\sum_{i=T+1}^{T-1} i.h(i)}{\omega_2}$$

12. GMAC

Global scale minimization of active contour model analyzes the implementation of it cell-image segmentation. This method is very easy to implement, it also has a relatively fast computation speed, and it cannot be stopped at a local minima. GMAC improves ACWE by dual formulation of the TV form and weighted total variation. GMAC is defined below,

$$\min E_{GMAC}(\mu, \lambda) := TV_g(\mu) + \frac{1}{20}\ \left|\ \right|\mu - v\ \Big|_{L_2}^2 + \lambda \int r_1(\text{x}, c_1, c_2)\ \mu + \alpha v(v)\ dx$$

where $r_1(x, c_{1,}c_{2)} = ((c_1 - f(x))^2 - (c_2 - f(x)^2 dx\, f(x)$ is the given image, and c_1 and c_2 are used for iteration of partition. e.g.:μ^*= arg min $E^2[\mu, v, c_1, c_2]$.

$$TV_g = \int g(x) \left| \nabla_\mu \right| \mathrm{dx}$$

where g(x) is a function that indicates an edge gives a link between region terms and snake model.

The equation below is the minimization equation that is solved until convergence:

$$c_1 = \frac{\int f(x)v(x)dx}{\int v(x)dx}$$

$$c_2 = \frac{\int f(x)(1-v(x))dx}{\int (1-v(x))dx}$$

$$p^{n+1} = p^n + \delta t \nabla div p^n \text{-(f-v)}/\theta / p^n + \nabla \frac{\delta t}{g(x)}$$

$$div p^n \text{- (f-v)}/\theta$$

$$\mu = v - \theta$$

$$\text{V(x) =min} \quad \{\max \mu(x) - \theta \lambda r1(x, c_1, c_2\ ), 0\}, 1\}$$

13. Microscopic cell clustering using K-means methodologies

Acknowledgment of white platelets (WBCs) is the initial step to analyze a few specific illnesses like AIDS, prostate, and other blood-related infections that are typically finished by pathologists utilizing an optical magnifying lens. This interaction is tedious, incredibly dreary, and costly and needs experienced specialists in this field. Accordingly, a PC supported analysis framework that helps pathologists in the analytic cycle can be so successful.

Division of WBCs is generally an initial phase in fostering a PC helped analysis framework. The primary motivation behind this work is to fragment WBCs from infinitesimal pictures. For this reason, we present a mix of thresholding, k-implies grouping, and adjusted AI calculations in three phases including division of WBCs from an infinitesimal picture, extraction of cores from cell's picture, and partition of covering cells and cores.

The assessment consequences of the proposed strategy show that closeness measures, accuracy, and responsiveness individually were 92.07, 96.07, and 94.30% for core division and 92.93, 97.41, and 93.78% for cell division. Moreover, measurable investigation presents high closeness between manual division and the outcomes got by the proposed technique.

14. Experimental setup and procedure

Below are the test results from division of three types of fluorescent pictures of cells: engineered cell pictures, cores pictures with ground truth, and synapse minute pictures. The initial two kinds of picture information are utilized to assess the performance of the four division techniques and to contrast the outcomes with the data. The synapse pictures are sectioned with subjective execution investigation because of the absence of ground truth.

Figure 3. Average measurements after segmentation is applied on the low quality synthetic cell images

	F-score	**Precision**	**Recall**
K-Means with EM	.9350	.9530	.9180

NB	.9041	.8268	.9987
Otsu's	.9739	.9799	.9678
GMAC	.9704	.9875	.9539

15. Quantitative measure

We utilize the customary accuracy, review, and F-score is taken as the quantitative measure. These actions are common procedures that are used to assess the nature of the division results against the expected values.

$$\text{Precision} = \frac{\#SR \cap GT}{\#SR}$$

$$\text{Recall} = \frac{\#(SR \cap GT)}{\#SR}$$

$$\text{F-score} = \frac{2.(\text{precesion.recall})}{\text{precesion+recall}}$$

16. Segmentation of synthetic data

The selected set is the subsequent benchmark set which comprises of multichannel cell pictures since we don't have appropriate genuine cell pictures with ground truth for assessment. Here, cores, cytoplasm, and sub cell parts have been mimicked by tuning boundaries like size, area, arbitrariness of shape, and other foundation or fluorescence boundaries. The picture sets are partitioned into two subsets: superior grade and bad quality, each comprising of twenty cell pictures. The subsequent set has covering cells and a boisterous foundation. Every picture contains fifty cells. As every picture is a reenacted picture has a relating paired veil as ground truth, twofold tasks can without much of a stretch compute the quantitative measure characterized previously.

Values for the division results utilizing sub cell pictures with top caliber. We see that the division aftereffects of lower quality pictures, with noisier foundations and covering cells, have more awful outcomes than those in great pictures. K-means, Otsu's limit and GMAC acquire comparable division quality in the two arrangements of pictures, estimated by Fscore, accuracy, and review. Their presentation is more strong against clamors than EM. Besides, EM calculations have lower accuracy, while keeping a lot higher values, particularly for the pictures of cells with boisterous foundations.

Figure 4. Average measurements after segmentation is applied on the low quality synthetic cell images

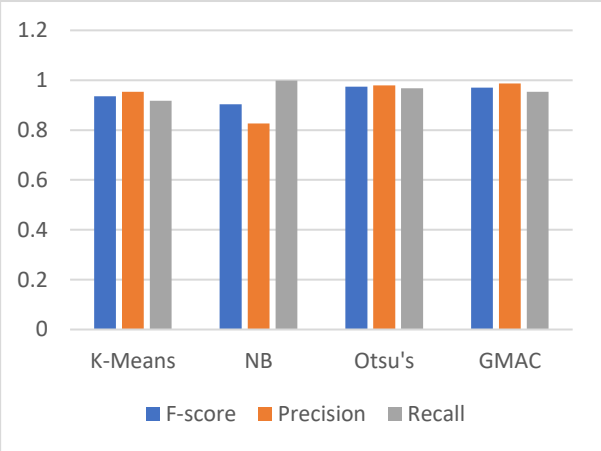

17. Results

The results indicate that K-Means Clustering and Naive Bayes do not score consistently when it comes to prediction. Whereas, Otsu's and GMAC (Global scale Minimization of Active Contour model) have consistently given better results. In the future, we also plan to make more alterations when it comes to the calculation methods. We shall soon try to utilize SVM and KNN model more efficiently in the upcoming work to decrease the number of steps when it comes to post-handling of data.

18. Conclusion

K-Means Clustering with Expectation Maximization method was used for cell division in fluorescent microscopy pictures. Very satisfactory results were received after

using this strategy. This strategy has proved to be efficient do identify the cell borders and make a partition between them so that they can be identified individually. To isolate the cells properly and with accuracy, splitting merch process has been used with the help of machine learning.

References

[1] K. Sklinda, M. Frnczek, B. Mruk, and J. Walecki, "Normal 3T MR life systems of the prostate organ and encompassing constructions," Adv. Drug., vol. 2019, pp. 1-9, May 2019.

[2] K. H. Hammerich, G. E. Ayala, and T. M. Wheeler, Anatomy of the Prostate Gland and Surgical Pathology of Prostate Cancer. Cambridge, U.K.: Cambridge Univ. Press, 2019, pp. 1-10.

[3] H. Ideo, J. Kondo, T. Nomura, N. Nonomura, M. Inoue, and J. Amano, "Study of glycosylation of prostate-explicit antigen emitted by malignant growth tissue-started spheroids uncovers new contender for prostate disease identification," Sci. Rep., vol. 10, no. 1, pp. 1-13, Dec. 2020.

[4] R. A. Mahumud, K. Alam, J. Dunn, and J. Gow, "The weight of ongoing illnesses among Australian disease patients: Evidence from a longitudinal investigation, 2007-2017," PLoS ONE, vol. 15, no. 2, Feb. 2020, Art. no. e0228744.

[5] N. M. Schultz, K. O'Day, R. Sugarman, and K. Ramaswamy, "Budget effect of enzalutamide for non-metastatic mutilation safe prostate malignant growth," J. Overseen Care Specialty Pharmacy, vol. 26, no. 4, pp. 538-549, Apr. 2020.

[6] M. B. Cook, D. C. Beachler, L. E. Parlett, P. T. Cochetti, W. D. Finkle, S. Paths, and R. N. Hoover, "Testosterone treatment comparable to prostate malignant growth in a us business protection claims data set," Cancer Epidemiol. Counteraction Biomarkers, vol. 29, no. 1, pp. 236-245, 2020.

[7] M. Wang, G. Chi, Y. Bodovski, S. L. Holder, E. J. Lengerich, E. Wasserman, and A. C. McDonald, "Temporal and spatial patterns and determinants of forceful prostate malignant growth among highly contrasting men with prostate disease," Cancer Causes Control, vol. 31, no. 1, pp. 63-71, Jan. 2020.

[8] P. C. Albertsen, J. A. Hanley, D. F. Gleason, and M. J. Barry, "Competing risk investigation of men matured 55 to 74 years at analysis oversaw safely for clinically limited prostate disease," Jama, vol. 280, no. 11, pp. 975-980, 2020.

[9] Y. Peng, Y. Jiang, C. Yang, J. B. Brown, T. Joke, I. Sethi, C. Schmid-Tannwald, M. L. Giger, S. E. Eggener, and A. Oto, "Quantitative investigation of multi-parametric prostate MR pictures: Differentiation between prostate disease and typical tissue and connection with Gleason score-A PC supported determination improvement study," Radiology, vol. 267, no. 3, pp. 787-796, Jun. 2018..

[10] M. Moradi, S. E. Salcudean, S. D. Chang, E. C. Jones, N. Buchan, R. G. Casey, S. L. Goldenberg, and P. Kozlowski, "Multiparametric MRI maps for discovery and evaluating of predominant prostate growths," J. Magn. Reson. Image., vol. 35, no. 6, pp. 1403-1413, Jun. 2019.